Controllable Growth of Bi_2MoO_6 Nanoplates by Citric Acid Assisted Hydrothermal Process and Their Photocatalytic Properties

WANG Yi[1, a]

[1]Tianjin Medical College, Tianjin 300222, P.R.China, [a]wangyii_2013@163.com

Abstract. Bi_2MoO_6 nanoplates with different sizes have been controllably fabricated by citric acid (CA) assisted hydrothermal process. The effects of CA on the morphology of Bi_2MoO_6 nanoplates have also been investigated. It is found that CA has a critical role in the crystallinity and size of Bi_2MoO_6 nanoplates. On the basis of XRD analysis and SEM observation of the products, the mechanism for CA assisted hydrothermal synthesis of the Bi_2MoO_6 nanoplates is discussed. The photocatalytic activity of as-prepared Bi_2MoO_6 was evaluated by the degradation of RhB dye in water, and the sample prepared when the amount of CA was 2.5mmol exhibited the highest photocatalytic activity.
Keywords: Bi_2MoO_6; hydrothermal process; citric acid

1 Introduction

Considerable research during the past few years has shown that photocatalytic decomposition of organic pollutants using semiconductors is a potential way of solving environmental issues. In the past few years, TiO_2 has been used extensively as photocatalyst for degradation of dyes in wastewater due to its high photocatalytic activity, low cost and nontoxicity. However, TiO_2 responds only to the ultraviolet light ($\lambda < 400$ nm) that accounts for only about 4% of the sunlight due to its wide band gap (3.2 eV). This limits the efficient utilization of solar energy for TiO_2 photocatalysis. Therefore, considerable effort has been made to design novel materials with narrow band gap.

Bi_2MoO_6 is one of the simplest members of the Aurivillius oxide family of layered perovskites with the general formula $Bi_2A_{n-1}B_nO_{3n+3}$ (A= Ca, Sr, Ba, Pb, Na, K; B=Ti, Nb, Ta, Mo, W, Fe; and n =number of perovskite-like layers $(A_{n-1}B_nO_{3n+1})^{2-}$),which are structurally composed of perovskite layers ($A_{n-1}B_nO_{3n+1}$) between bismuth oxide layers (Bi_2O_2)[1,2], Dielectric[3], ion conductive[4,5], and catalytic properties[6] of this material have attracted attention. Recently, it has also been reported that Bi_2MoO_6 is a good photocatalyst for water splitting and photodegradation of organic compounds under visible light irradiation[7-9]. It is well-known that the photocatalytic activity closely relates with the particle size, surface areas, the efficiency of electron-hole separation, etc., of the photocatalysts. Thus, the synthesis of Bi_2MoO_6 photocatalysts with controlled microstructure is a subject of considerable research interest.

In this paper, we report the controllable growth of Bi_2MoO_6 nanostructures by citric acid (CA) assisted hydrothermal process.The photodegradation of Rhodamine B (RhB) was

employed to evaluate the photocatalytic activities of Bi_2MoO_6, Moreover,the mechanism for the CA assisted hydrothermal synthesis of Bi_2MoO_6 nanostructures has been discussed.

2 Experimental and Methods

2.1 Synthesis of the Samples

In a typical synthesis,5.0mmol of $Bi(NO_3)_3 \cdot 5H_2O$ was dissolved in 15 mL of diluted HNO_3 solution, then the weighed amount of citric acid was added to this solution , the amount of CA were 1.0, 2.5, 4.0, 5.0mmol for samples S1, S2, S3 and S4. Meanwhile, 2.5mmol $Na_2MoO_4 \cdot 2H_2O$ was dissolved in 15ml deionized water. The two solutions were mixed under vigorous stirring and the pH was adjusted to 7.0 by NaOH solution(2M). This precursor solution was poured into a 60ml Teflon-lined stainless steel autoclave, and then heated at 180℃ for 24h. After the autoclave was cooled to room temperature, the precipitate was separated by centrifugation, washed several times with deionized water and ethanol, and dried in an oven at 80°C for 12 h.

2.2 Characterization

The X-ray diffraction (XRD) patterns were recorded on a Rigaku D/max 2500 diffractometer with Cu-Kα radiation at a scanning speed of 8°/min ranging from 20 to 60°. The scanning electron microscope (SEM) characterizations were performed on a Nanosem 430 field emission scanning electron microscope.The UV-vis absorption spectra were measured on Shimadzu UV-2550 spectrophotometer using $BaSO_4$ as a reference in wavelength of 200–800 nm.

2.3Photocatalytic Test

Photocatalytic activity of the obtained Bi_2MoO_6 samples was investigated by photocatalytic degradation of rhodamine B(RhB) under a 300 W tungsten halogen lamp (Philips Q/YXKC33). 0.1g of the prepared photocatalyst was added to 100 mL aqueous solution of 1×10^{-5}mol/L RhB. Before illumination, the suspensions were magnetically stirred in the dark for 60min to ensure the establishment of an adsorption-desorption equilibrium between the photocatalysts and RhB.At given time intervals,3ml aliquots were sampled and centrifuged to remove photocatalyst powders. The concentration of centrifugated solution was determined by measuring the absorbance value at approximately 553 nm.

3 Results and Discussion

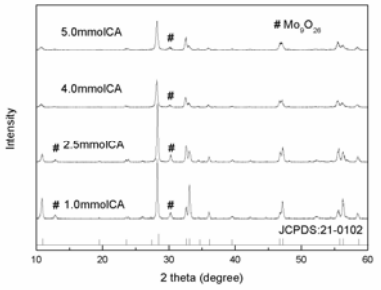

Fig.1 XRD patterns of the as-prepared Bi_2MoO_6 samples

Fig.1 shows the XRD patterns of the as-prepared Bi_2MoO_6 samples. All the diffraction peaks can be indexed to Bi_2MoO_6 (JCPDS No. 21-0102), but with a small impurity that was identified as Mo_9O_{26} (JCPDS Card No. 65-1292). It is also found that the intensity of diffraction peaks decreases when the amount of CA exceeds 2.5mmol, indicating crystallinity becomes worse. The average crystallite sizes of the samples were calculated to be 61.7, 50.4, 33.8, 30.3nm for sample S1, S2, S3 and S4, respectively.

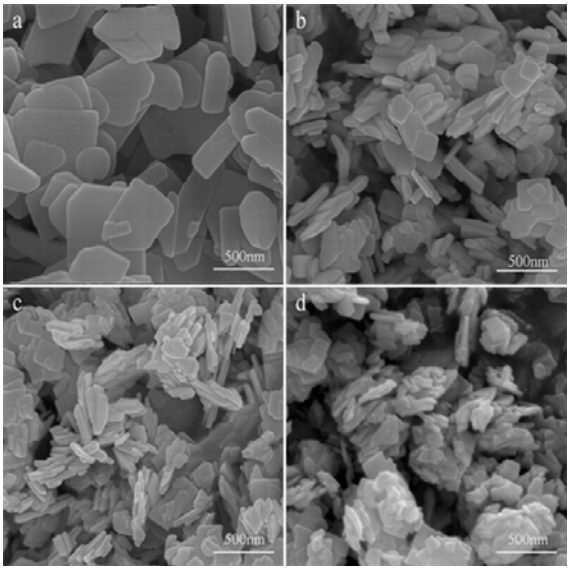

Fig.2 SEM images of Bi_2MoO_6 samples prepared by hydrothermal method with different amount of citric acid. (a)1.0mmol(b) 2.5mmol(c) 4.0mmol(d) 5.0mmol

Fig.2 shows SEM images of Bi_2MoO_6 samples prepared by hydrothermal method with different amount of citric acid. As can be seen, all the products are composed of nanoplates and the dosage of citric acid has a significant impact on the size of the as-synthesized products.The average size of nanoplate decrease with increasing the amount of citric acid. While the amount of citric acid was increased from 1.0mmol to 2.5mmol, the size of Bi_2MoO_6 nanoplates become smaller and more uniform.When the the amount of citric acid was 4.0mmol, the size of Bi_2MoO_6 nanoplates futher decrease and aggregate slightly.When the amount of citric acid was further increased to 5.0mmol, nanoplates aggregate compactly together. Based on XRD and SEM results, we suggested that the optimum dosage of citric

acid was 2.5mmol.

It is well known that citric acid can be used used as complexing agent and can form strong complexes with metal ions through a coordination interaction[10]. It can also adsorb strongly on metal and mineral surfaces, significantly alter their surface properties and mineral growth behavior. In our experiment, the free Bi^{3+} ion concentration would decrease in solution because Bi^{3+} ions with citrate groups can formed complexes, the free Bi^{3+} ion concentration have a great impact on the nucleation and growth rate of Bi_2MoO_6, thus, the nucleation and growth rate of Bi_2MoO_6 can be controlled through changing the amount of citric acid. As the temperature increased during the hydrothermal reaction, the chelation of the Bi^{3+}-citrate complex would be weakened and Bi^{3+} would be released gradually. Therefore, the nucleation and growth of Bi_2MoO_6 will go through a longer process, which is helpful to form uniform crystals.

On the basis of the experimental results and observations,the possible reactions carried out are proposed as follows:

$$Bi(NO_3)_3 \leftrightarrow Bi^{3+} + 3NO_3^- \quad \text{(a)}$$

$$Na_2MoO_4 \leftrightarrow 2Na^+ + MoO_4^{2-} \quad \text{(b)}$$

$$Bi^{3+} + C_6H_5O_7^{3-} \leftrightarrow C_6H_5O_7Bi \quad \text{(c)}$$

$$C_6H_5O_7Bi \leftrightarrow Bi^{3+} + C_6H_5O_7^{3-} \quad \text{(d)}$$

$$2Bi^{3+} + MoO_4^{2-} + 2H_2O \rightarrow Bi_2MoO_6 + 4H^+ \quad \text{(e)}$$

As shown in Formula a, when $Bi(NO_3)_3 \cdot 5H_2O$ was added into diluted HNO_3 solution, Bi^{3+} will be produced and MoO_4^{2-} will be produced when Na_2MoO_4 dissolves in water (Formula b). After the dissolution of CA, $Bi^{3+}$was transformed into a $C_6H_5O_7Bi$ as a result of the strong coordination action of Bi^{3+} with citric anions, as shown in formula c. When these two solutions are mixed, a white precipitate of Bi_2MoO_6 will be immediately produced. The mixture became more and more clear with increasing the amount of CA. When the amount of CA was increased to 5.0mmol (Bi/CA=1:1), the mixture became transparent, that is because Bi^{3+} will not directly react with MoO_4^{2-} to produce the precipitate Bi_2MoO_6 due to the coordination of Bi^{3+} with citric anions. Under hydrothermal conditions, as the temperature increased, the $C_6H_5O_7Bi$ would gradually decompose and slowly release Bi^{3+}, followed by the reaction with MoO_4^{2-}, as shown in formulas (d) and (e). Thus, the nucleation and growth process of Bi_2MoO_6 is tuned during the hydrothermal process. As a result, Bi_2MoO_6 with smaller size is obtained.

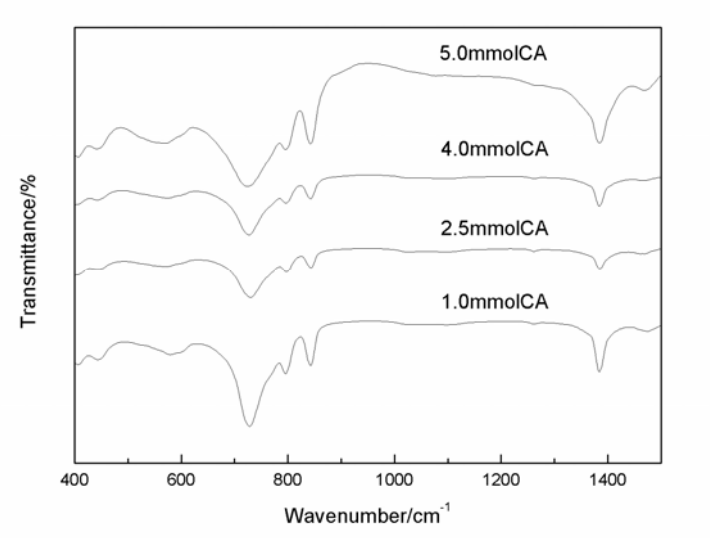

Fig.3 FT-IR spectra of as-synthesized Bi_2MoO_6 products

Fig.3 shows FT-IR spectra of as-synthesized Bi_2MoO_6 products. The bands at around 843 and796 cm^{-1} can beassigned as the asymmetric and symmetric stretching mode of MoO_6 involving vibrations of the apical oxygen atoms,respectively.The band at 728 cm^{-1} is attributed to the asymmetric stretching mode of MoO_6 involving vibrations of the equatorial oxygen atoms[11]. The bands in the 600–400 cm^{-1} range are assigned to Bi-O stretching vibration and deformation vibration.

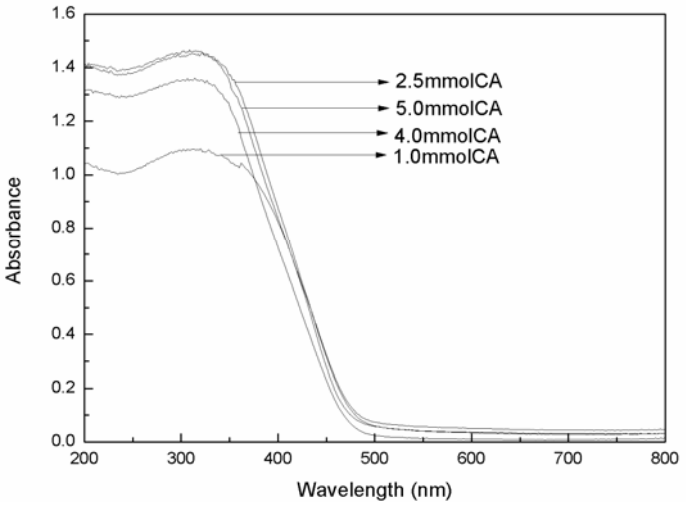

Fig.4 UV-vis diffuse reflectance spectra of the as-synthesized Bi_2MoO_6 samples

Optical absorption of the Bi_2MoO_6 nanoplates was measured by using an UV–vis spectrometer. The UV-vis diffuse reflectance spectra of the as synthesized Bi_2MoO_6

samples is shown in Fig.4. The band gap absorption edge of all these samples is estimated to be about 483 nm, corresponding to a band gap energy of about 2.57 eV. The steep shape of the spectra indicates that the light absorption is not due to the transition from the impurity level but is due to the band-gap transition[12, 13]. The band structure of Bi_2MoO_6

is suggested to be composed of Mo 4d orbitals with Bi 6p orbitals for the conduction band and O 2p orbitals for the valence band. The main orbitals comprising the conduction band are Mo 4d orbitals rather than Bi 6p orbitals. It is revealed that the visible-light absorption of Bi_2MoO_6 was due to the transition from the valence band consisting of the O 2p orbitals to the conduction band derived from the primary Mo 4d orbitals in MoO_6 octahedra and the secondary Bi 6p orbitals[14].

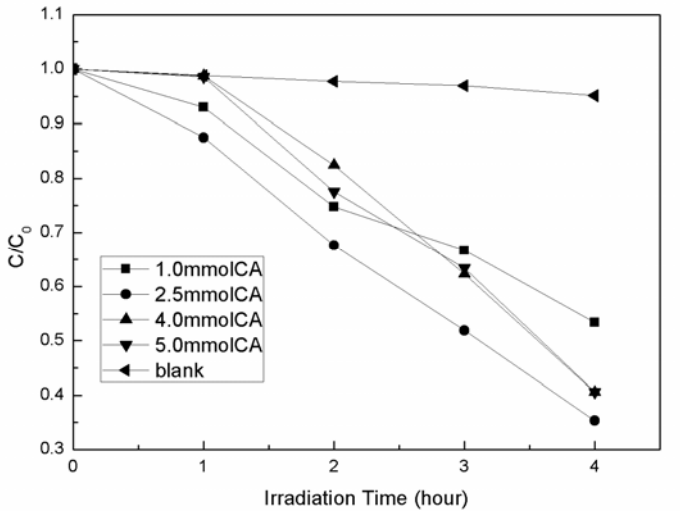

Fig.5 The photodegradation of RhB dye as a function of irradiation time

Fig.5 showed the efficiencies of the photocatalytic degradation in the presence of Bi_2MoO_6 samples, C was the absorption of RhB at the wavelength of 553nm and C_0 was the absorption after the adsorption equilibrium on Bi_2MoO_6 before irradiation. Blank test (RhB without any catalyst) under tungsten halogen lamp exhibited little photolysis.It is clearly seen that the dosage of CA have significant effects on the degradation rate of photocatalysts. When the amount of CA was 2.5mmol, the Bi_2MoO_6 nanoplate possessed the best photocatayltic activity, the amount of CA was futher increased, photocatayltic activity decreased.

It is well known that the photocatalytic activities are closely related to their crystallinity and surface areas[15]. A high degree of crystallinity and a large surface area are favorable to the photocatalytic performance due to fewer defects acting as electron–hole recombination centers and more active sites in the photocatalytic process. Compare to sample S1, the sample S2 have smaller particle size, so the surface area of sample S2 maybe higher than that of sample S1, which was advantageous to its photocatalytic activities. The particle size of Sample S3 and sample S4 are smaller than that of sample S2, but their crystallization are not good enough which could be observed from the XRD results,This imperfect crystallization is considered to favorably increase the probability of electron–hole recombination, which is unfavorable to the photocatalytic performance.Therefore, the photocatalytic activities of the samples S3 and S4 decreased and the sample S2 possessed the best photocatayltic activity.

4 Conclusions

In conclusion, CA could be used as a complexing agent to control the nucleation and growth rate of Bi_2MoO_6, the amount of CA in CA assisted hydrothermal process have been found to have a significant influence on the morphology of Bi_2MoO_6 nanoplates. The

average size of nanoplate decrease with increasing the amount of CA, which may lead to higher specific surface area and photocatalytic activities, but the crystallinity decreased, which is unfavorable to the photocatalytic activities.Therefore, the amount of CA may have one optimum value, in our experiments, Bi_2MoO_6 prepared when the amount of CA was 2.5mmol exhibited the highest photocatalytic activity. This method has the potential use in preparation of other bismuth compound photocatalysts.

Acknowledgement

We gratefully acknowledge financial support by the National Natural Science Foundation of China (Grant No. 41201487)

References

1. **Y. Tsunud**a, W. Sugimoto and Y. Sugahara, *Chem.Mater.*,2003, 15, 632-635.
2. J. X. Xia, H. M. Li and Z. J. Luo, *Materials Chemistry and Physics*, 2010, 121, 6-9.
3. M. Hartmanova, M. T. Le and I. Driessche, *Russian Journal of Electrochemistry*, 2005, 41, 455-460.
4. R. Murugan, Physical B: *Candensed Matter*, 2004, 352, 227-232.
5. L. T. Sim, C. K. Lee and A. R. West, *J. Mater. Chem.*, 2002, 12, 17-19.
6. J. C. Lun, H. Kim and Y. S. Kim, *Applied Catalyst A:General*, 2007, 317, 244-249.
7. J. Q. Yu and A. Kudo, *Chemistry Letters*, 2005, 34, 1528-1529.
8. H. H. Li, C. Y. Liu and K. W. Li, *Journal of Material Science*, 2008, 43, 7026-7034.
9. W. Z. Yin, W. Z. Wang and S. M. Sun, *Catalysis Communication*, 2010, 11, 647-650.
10. D. K. Ma, S. M. Huang and W. X. Chen, *J. Phys. Chem. C*, 2009, 113, 4369-4374.
11. L. Zhang, T. Xu and X. Zhao, *Applied Catalysis B: Environmental*, 2010, 98, 138-146.
12. A. Kudo and M. Sekizawa, *Chem. Commun.*, 2000, 15, 1371-1372.
13. A. Kudo and M. Sekizawa, *Catal. Lett.*, 1999, 58, 241-243.
14. Y. Shimodaira, H. Kato and H. Kobayashi, *J. Phys. Chem.* B, 2006, 110, 17790-17797.
15. J. G. Yu, J. F. Xiong and B. Chen, *Journal of Solid State Chemistry*, 2005, 178, 1968-1972.